Wireless Power Transfer for Bluetooth Low Energy Based IoT Device: an Empirical Study of Energy Performance

Diluna Adeesha Warnakulasuriya, Konstantin Mikhaylov, Onel L. Alcaraz López
Centre for Wireless Communications
University of Oulu
Oulu, Finland
{dwarnaku22@student.oulu.fi, konstantin.mikhaylov@oulu.fi, onel.alcarazlopez@oulu.fi}

***Abstract*—Radio Frequency (RF) Wireless Power Transfer (WPT) is a prospective technology promising to enable uninterrmittent and maintenance-free operation of IoT devices. In this paper, we shed some light on the energy performance of the state-of-the-art RF-WPT in Bluetooth Low Energy (BLE) and IoT hardware platforms, specifically the Powercast P21XXCSR-EVB and the Texas Instruments CC2652R1 multi-radio protocol system-on-chip. For this, we first study the energy consumption of the CC2652R1 communicating over BLE technology in advertising mode, and the effect of the different BLE configuration parameters, such as transmit power, the number of channels, advertising interval and size of advertising packet, have on the energy consumption. Next, we investigate how much energy can be harvested and stored in the P21XXCSR-EVB, when RF transmission is from a dedicated WPT equipment. Finally, we integrate both elements to instrument a WPT-powered IoT device communicating over BLE, and investigate its energy consumption. Our results show the feasibility of instrumenting a WPT-powered IoT device today, while revealing some challenges and limitations of this approach. We believe that our results can be a reference for new designs, further optimizations and analytic/simulation models for WPT-powered IoT.**

***Index Terms*—Wireless Power, Energy, WPT, IoT, BLE, experiment, measurement**

I. Introduction

The number of Internet of Things (IoT) devices grows at an ever-increasing rate, making their service and energy supply especially challenging. To address this, IoT devices may incorporate novel capabilities in terms of energy harvesting from, e.g., light, heat, or Electromagnetic (EM) fields, instead of charging wires and traditional batteries. Since ambient energy availability is often opportunistic, which may cause intermittent operation of the IoT applications depending on the energy supply method, dedicated Wireless Power Transfer (WPT) technology has gained more interest recently [1]. Specifically, radio frequency (RF) WPT, herein referred to simply as WPT, suggests delivering energy from a power supply to the target through the air over distances in the order of tens of centimeters to a few meters [2]. Even though the concept looks very attractive, this technique's key challenge lies in the massive energy loss in the wireless channels.

Noteworthy, whether IoT devices are powered by ambient energy harvesting or WPT, their energy consumption should be optimized. Because high power consumption can negatively impact the user experience and the device's intended purpose. Indeed, optimizing the energy consumption for communication, which often constitutes a substantial part of the energy budget, is crucial here. Therefore, one of the most crucial design aspects lies in properly selecting the radio access technology. As of today, Bluetooth Low Energy (BLE) offers short-range wireless connectivity characterized by low power consumption and low transceiver costs. Based on this, herein, we discuss and study using empirical methods the feasibility of using WPT for charging BLE-enabled IoT devices by considering the energy consumption prospective and the different communication and operation modes' effect. Specifically, we first characterize the impact of transmit power, number of channels, payload length, and advertising interval on the energy consumption of the BLE communication using Texas Instruments (TI)[1] CC2652R1 chips. Next, we investigate how much energy can the Powercast[2] P21XXCSR-EVB harvest and store when it is placed at different distances from a 3 W WPT transmitter operating in the 880-928 MHz range. Finally, we integrate these two elements, thus creating a WPT-powered BLE-based IoT device, and assess the system's energy performance. The structure of our WPT-BLE setup is illustrated in Fig. 1. Our results experimentally validate and show today's WPT-enabled IoT capabilities, providing experimental inputs (e.g., concerning energy consumption in different modes or WPT efficiency) that are relevant for further analysis and modeling of such systems and the applications based on them. We hope that our results and the lessons learned benefit and boost the design of novel IoT products based on the WPT concept.

The rest of the paper is organized as follows. In Section II, the literature related to our work is discussed. The experimental setup, including the details about the Hardware (HW) and the experiment procedures, are presented in Section III. Section IV reveals the measurement results and their analysis. Finally, Section V concludes the paper and summarizes the

[1]https://www.ti.com/
[2]https://www.powercastco.com/

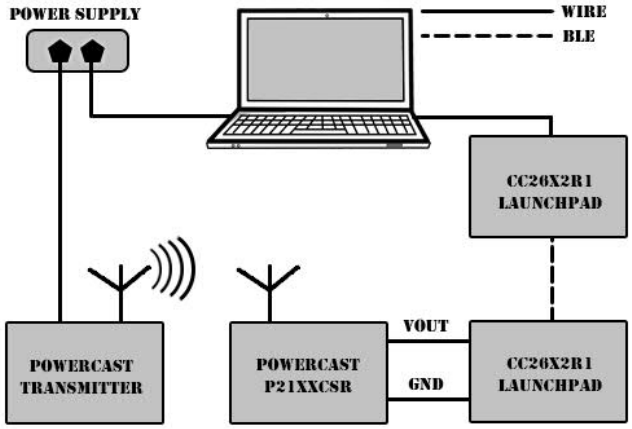

Fig. 1. Illustration of WPT-BLE system

key outcomes.

II. Related works

In recent years, several studies have focused on WPT using RF based Energy Harvesting (EH), which denotes a mechanism whereby rectifying antennas are employed to capture EM signals emitted from nearby sources (e.g., mobile phones, TV signals, or radio stations) and convert to usable Direct Current (DC) voltage [3]. In the rest of this section, we focus our discussion on recent studies relying on dedicated WPT summarized in Table I, while we discuss their key aspects in the following.

The study [3] used Powercast P1110 and P2110 energy harvesters, showing that the former has a higher RF-to-DC conversation efficiency at the same transmission range. Some authors have also investigated the effect of the antenna type [4], [5] and storage capacitors [2] for Powercast P21XXCSR-EVB. Meanwhile, the authors in [2], [6], [7] employed the WPT system using the Powercast energy harvesters to prototype various BLE beacons, sensor nodes, and ZigBee applications.

Note that the previously discussed studies leveraged energy harvesting from an unmodulated carrier wave. Contrary, the research reported in [7] investigated RF energy harvesting from a packet-based network. Interestingly, unlike carrier waves, packet-based communications may lead to some idle time in between transmissions of packets, during which energy is not transferred. The study showed the effect of packet size and other parameters on energy transfer efficiency.

The effect of the operating environment on the WPT efficiency was investigated in [4]. Specifically, the authors characterized the RF energy harvesting efficiency in two distinct test environments: the outdoor free-field and the indoor reverberate. They show that there is a regular trend of harvester charging time and RSSI in the outdoor free field scenario, while irregular trends inside the rooms with reflective walls. Meanwhile, [7] focused on the effect of the interference on the WPT efficiency. Interestingly, the interference, being a form of energy itself, can harm the RF based energy harvesting efficiency by disrupting the (optimized) waveform of the incoming signals [7].

TABLE I
Related Works

Ref.	Main scope of the research
[2]–[5]	Study on the RF energy harvesting performance using Powercast P1110/P2110 for long range and short range transmission.
[6], [8]	Analysis of the energy harvested by a Powercast node for BLE beacon and ZigBee applications.
[9]	Comparison of the energy consumption of various BLE versions and the effect of connection interval, read/write transactions, and data volumes on energy consumption.
[4]	Evaluation of the variation of time taken by PowerCast energy harvester for charging and the Received Signal Strength (RSSI) captured by PowerCast energy harvester along the spatial coordinates.
[7]	Experimental study on RF-based Simultaneous Wireless Information and Power Transfer (SWIPT) techniques using Powercast P2110.
[10]	Comparison of waveforms such as Orthogonal Frequency-Division Multiplexing (OFDM), square, triangular, sinusoidal, and Sawtooth for a suitable WPT mechanism using Powercast P21XXCSR-EVB.
[11]	Study the WPT-BLE communication in a moving envirnoment for battery-less asset tracking modules.

A few studies have also prototyped various applications based on the WPT concept. A battery-less BLE tag powered by WPT for asset tracking in a moving environment is presented in [11]. A BLE Integrated Circuit of the tag was configured to transmit non-connectable, undirected advertising mode, with an advertising data packet of 32 bytes and an output power of -14 dBm. Although WPT systems may sound less suitable for aviation use cases, the authors of [11] suggested and showed a WPT for low-power cabin sensors onboard an aircraft.

Many existing studies in the broader literature have examined the performance of energy harvesting technology using Powercast energy harvesters for WPT. Most authors have considered parameters like input signal strength, distance between transmitter and receiver, and different size storage capacitors for their experiments. Also, there are some papers regarding the energy consumption of BLE, ZigBee and beacon applications. However, studies investigating the design of WPT-enabled BLE applications are mostly absent to this date. The existing researches have many problems in representing energy consumption profiles for different configurations of BLE. Therefore, in this study, we approach this gap and first investigate the effect of the BLE communication parameters and traffic patterns on the energy consumption of an IoT device and then study how well such an IoT device can be powered via WPT.

III. Experimental setup

The key HW and Software (SW) components used in our study are listed in Table II. In the three following subsections, we first discuss in details the BLE and WPT components as standalone, and then the integrated WPT+BLE IoT device. Also, we detail the procedure for our measurements.

TABLE II
UTILIZED HARDWARE AND SOFTWARE

Device/software Role	Model No/Name	Vendor
WPT receiver	P21XXCSR-EVB	Powercast
WPT receiver's antenna	MAF94300	TE Connectivity
WPT transmitter	TX91501	Powercast
BLE Transmitter	LAUNCHXL CC26X2R1	Texas Instruments
BLE Receiver	LAUNCHXL CC26X2R1	Texas Instruments
IDE	Code Composer Studio	Texas Instruments
BLE Sniffer SW	RF Packet Sniffer WireShark	Texas Instruments WireShark

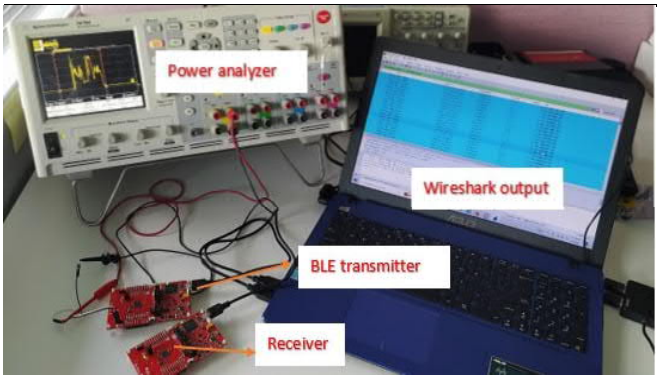

Fig. 2. Illustration of the measurement setup for BLE power consumption

A. BLE - Bluetooth Low Energy

First, we characterize the energy consumption of a BLE device transmitting data in advertising mode and the effect of different configuration parameters on it. The reason for focusing on the advertising mode operation is because this mode is characterized by lower signaling overhead and higher flexibility, and is widely used by contemporary IoT devices (e.g., beacons or various broadcasting sensors). Therefore, we consider this mode to be more prospective for WPT-powered BLE device operation than a connection-based one.

The experimental setup is illustrated in Fig. 2. It is composed of four main components: (i) one CC26X2R1 launchpad BLE board with an integrated antenna, whose consumption is being measured, (ii) the Agilent N6705B DC power analyzer, (iii) a second CC26X2R1 launchpad connected to a laptop and acting as a BLE sniffer to ensure the correct operation of the transmitter (i).

For our tests, we program one of the CC26X2R1 Launchpad boards with the *simple peripheral* code using CCS IDE software. Note that TI provides several example codes under this specific device model software development Kit (SDK). Here, we slightly change the *simple peripheral* example given in *SimpleLink CC13x2 26x2 SDK (5.20.00.52)* version in order to specify the configuration parameters of interest, namely advertising interval, the number of channels, transmit power, and advertising data contents.

To measure the current consumption of the CC26X2R1 Launchpad, we use the Agilent N6705B DC power analyzer. Using cables, we connect the power analyzer to the microcontroller 3V3 (supply) and ground pins and measure the current

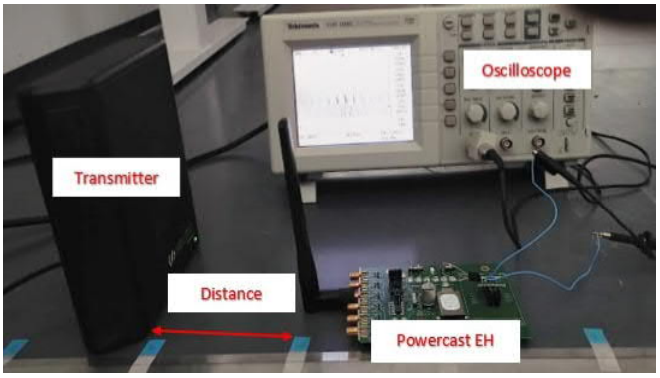

Fig. 3. Illustration of the measurement setup for the WPT performance

consumption in data logger mode. We configure the power analyzer to provide a 3.3 V constant voltage supply. Observe that the data logger mode is a valuable option available in the DC power analyzer, which allows getting the output in a CSV file format. We use these outputs for further analysis and calculations using MATLAB.

Since we are only interested in the non-connection state BLE transmission, we use *Non-connectable and Non-scannable undirected* legacy advertising mode. We consider 36 different scenarios, which are obtained by varying four parameters: (i) the advertising interval (either 100 ms or 1000 ms), (ii) the number of frequency channels (1, 2, and 3), transmit power (0 dBm, 5 dBm (the maximum supported by this radio), -20 dBm (the minimum supported by this radio)), and (iv) the physical layer payload size (23 or 49 bytes).

The second CC26X2R1 launchpad BLE board connected to a laptop is controlled by the RF packet sniffer software. The board captures the BLE radio packets and streams them through the *Pipe output* interface to Wireshark. Analyzing these allows us to ensure a correct operation of the transceiver, while we obtain information about the number of packets that are received and their timestamp.

B. WPT - Wireless Power Transfer

The WPT chain comprises the WPT transmitter and WPT receiver. As a transmitter, we adopt the Powercast TX91501b WPT transmitter with an integrated antenna operating in the 915 MHz band and transmitting carrier waves with transmit power of 3 W. As a receiver, we adopt the Powercast P21XXCSR-EVB board. This board supports energy harvesting from different frequency bands (GSM-850 uplink, Europe RFID GSM-850 downlink, ISM USA GSM-900 uplink, GSM-1800 uplink, GSM-1900 uplink, and Wi-Fi 2.4GHz.), and an optional storage of the collected energy in one of two capacitors. Moreover, the accumulated energy can be obtained through a regulated 3.3 V output. We depict the overall measurement setup for EH performance over distance in Fig. 3. During the measurements, we keep the RF transmitter at one constant point and move the Powercast EH away from it with 10 cm steps. Two different measurements are carried out as described next.

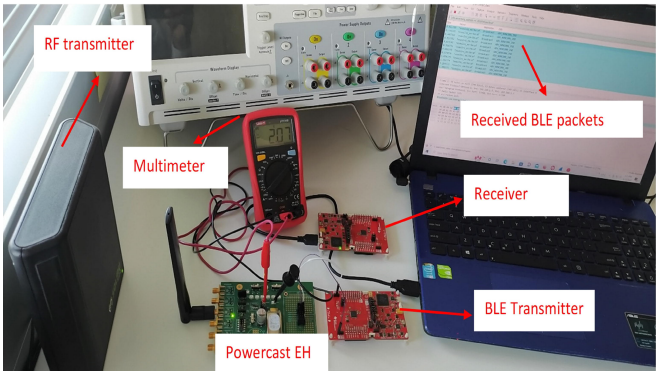

Fig. 4. Measurement setup for integrated WPT+BLE system

First, we measure the collected power by using a digital oscilloscope to measure the voltage on a resistor connected between WPT receiver's VOUT and GND pins. At this stage, we remove the JP1 jumper so that no capasitor is charged and all the collected energy goes to output. S1 and S3 switches are left in "default" (thus resulting in 3.3 V output) and "VCC/MEAS" states, respectively. The switch S2 is kept in the "OFF" position.

Second, we study how effectively the WPT process replenishes the energy in the two P21XXCSR-EVB capacitors. For this, we measure the voltage across the selected (with JP1) capacitor using the digital oscilloscope by connecting the probe between VCAP and GND pins. Note that during these measurements no load has been connected to the voltage output and the capacitors were fully discharged (by temporarily connecting an external load) prior to taking each measurement.

C. Integrated WPT + BLE

Finally, we combine the above discussed devices together. Specifically, we disable the supply of the CC26X2R1 Launchpad from USB by removing the jumpers (i.e., RESET, 3V3 voltage, 5V voltage, and XDS Power) and use the Powercast P21XXCSR-EVB board to power it instead. Note that the Powercast P21XXCSR-EVB device has two onboard capacitors with the possibility of using one more external capacitor. In this experiment, we use only the two onboard capacitors with 2200 μF and 50 mF capacitance. Also, the 1.2 V threshold is selected via JP3 of the EH device. The charger charges the selected capacitor up to this voltage, after which the boost converter is activated. The regulated voltage (selected by the S1 jumper; 3.3 V in our case) is provided on the VOUT.

In our first measurement, the capacitor is charged until it reaches at least 2.0 V voltage, and then the RF input is turned off. Then, we connect the EH to the BLE device, which sends advertising packets. This BLE operation is performed until the capacitor voltage reaches its minimum threshold value. In this way, we measure how long we can do the BLE transmission until the capacitor discharges from its steady state. For these measurements, we only consider the 100 ms advertising interval scenario. Likewise in the BLE-only tests, the other BLE board with Wireshark software is used to monitor and capture the BLE packets.

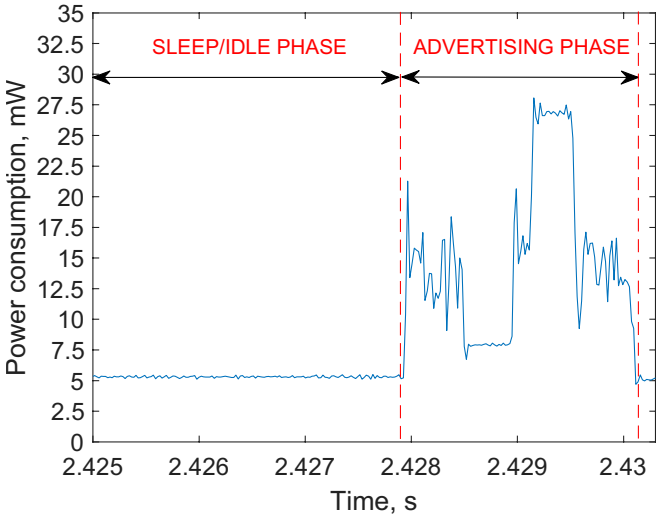

Fig. 5. Illustration of sleep and advertising phases of a BLE IoT device operation (sample of a captured BLE packet transmitted using a single advertising channel, 0 dBm TX power and the maximum advertising data at 100ms advertising interval.)

In our second measurement, we investigate the operation of the WPT supplied BLE IoT device in a long run. For this, we provide a continuous WPT supply to the BLE device and observe the periods of activity and inactivity of the IoT device (by observing its transmitted packets).

IV. Selected Measurement Results

This section illustrates selected experimental results obtained from the above experimental setups. Specifically, we present the results for CC26x2R1 LaunchPad power consumption followed by the harvesting efficiency of P21XXCSR-EVB device. Finally, we illustrate energy consumption results for the completely wirelessly powered low power BLE device.

A. BLE consumption measurement results

Fig. 5 illustrates the consumption profile during one exemplary BLE packet transmission. Generally, the consumption profile consists of two main phases: the sleep/idle phase and the advertising phase. The duration of the sleep/idle phase is substantially longer than the length of the advertising state. The average sleep/idle consumption is about 5.6 mW. Note that the default sleep/idle mode, as implemented in the *simple peripheral* example of *SimpleLink CC13x2 26x2 SDK (5.20.00.52)*, does not disable all the peripherals, resulting in decently high consumption. The advertising phase comprises several sub-phases (pre-processing, radio preparation, etc. [12]), characterized by different levels of energy consumption. We can observe that the highest consumption is above 27 mW during the actual transmission.

We measure the power consumption of the TI CC26x2R1 Bluetooth MCU device under different BLE configuration parameters. Table III summarizes the key metrics concerning energy consumption and duration for the advertising and

TABLE III
TI CC2652R1 BLE ENERGY CONSUMPTION MEASUREMENT RESULTS

Number of CH			TX Power (dBm)			Packet size		When Advertising Interval is 100ms										When Advertising Interval is 1000ms									
								Advertising			Sleeping		Total		Duration (ms)			Advertising			Sleeping		Total		Duration (ms)		
1	2	3	0	5	-20	Min	Max	Energy (uJ)	Power (mW)	Peak Power (mW)	Energy (uJ)	Power (mW)	Energy (uJ)	Power (mW)	Advertising	Sleep	Energy (uJ)	Power (mW)	Peak Power (mW)	Energy (uJ)	Power (mW)	Energy (uJ)	Power (mW)	Advertising	Sleep
✓			✓			✓		31.611	15.53	30.46	579.139	5.61	57853.54	5.79	2.036	103.298	31.585	15.47	29.94	5620.447	5.61	56259.86	5.63	2.041	1002.34
✓			✓				✓	38.113	17.12	27.92[1]	579.369	5.61	57866.91	5.81	2.226	103.274	37.993	16.85	29.91	5621.514	5.61	56301.52	5.63	2.254	1002.68
✓				✓		✓		33.134	16.25	37.74	578.209	5.60	57939.89	5.79	2.039	103.221	33.173	16.19	37.56	5627.131	5.61	56285.12	5.63	2.051	1003.34
✓				✓			✓	41.067	18.29	37.64	579.874	5.61	58573.95	5.86	2.246	103.441	41.134	18.21	37.51	5635.034	5.61	56365.87	5.64	2.258	1004.46
✓					✓	✓		29.885	14.62	21.18	577.096	5.60	57670.24	5.77	2.044	102.984	29.866	14.61	21.14	5621.808	5.61	56263.91	5.63	2.045	1002.22
✓					✓		✓	34.151	15.23	21.15	579.564	5.61	57984.38	5.81	2.242	103.348	41.049[1]	18.18[1]	37.48[1]	5625.171	5.61	56378.71	5.64	2.258	1002.46
	✓		✓			✓		40.822	16.77	30.07	575.224	5.61	58501.72	5.85	2.434	102.605	40.874	16.73	30.07	5617.693	5.61	56348.21	5.63	2.443	1001.49
	✓		✓				✓	53.431	18.71	29.99	573.201	5.61	59460.32	5.95	2.856	102.235	53.319	18.67	29.96	5620.371	5.60	56403.39	5.64	2.856	1002.75
	✓			✓		✓		43.764	17.98	37.88	577.115	5.60	58748.88	5.87	2.433	102.973	43.887	17.85	37.95	5621.051	5.61	5636.75	5.64	2.459	1002.25
	✓			✓			✓	59.528	20.87	37.86	574.428	5.61	60017.61	6.01	2.853	102.448	59.579	20.81	38.03	5613.329	5.61	56478.86	5.65	2.865	1001.19
	✓				✓	✓		37.287	15.29	21.18	575.258	5.60	58154.47	5.82	2.438	102.663	37.322	15.28	21.18	5614.218	5.61	56316.87	5.63	2.443	1000.84
	✓				✓		✓	46.024	16.13	21.12	569.522	5.61	58775.16	5.88	2.853	101.606	59.541[1]	20.72[1]	37.86[1]	5615.067	5.61	56514.76	5.65	2.873	1000.85
		✓	✓			✓		49.661	17.62	30.08	574.381	5.61	59123.18	5.91	2.818	102.468	50.052	17.52	29.93	5627.755	5.61	56464.17	5.65	2.856	1002.42
		✓	✓				✓	68.614	19.82	29.99	570.737	5.60	60557.31	6.06	3.463	101.828	68.617	19.75	29.99	5622.893	5.61	56579.43	5.66	3.475	1002.13
		✓		✓		✓		54.419	19.18	38.06	572.123	5.60	59540.81	5.95	2.837	102.075	54.461	19.07	38.00	5635.473	5.61	56483.47	5.65	2.856	1004.19
		✓		✓			✓	77.901	22.51	38.11	571.141	5.61	61468.88	6.15	3.461	101.788	77.824	22.47	38.11	5619.893	5.61	56625.09	5.66	3.463	1002.37
		✓			✓	✓		44.778	15.78	21.27	575.172	5.61	58655.09	5.87	2.838	102.613	44.786	15.75	21.27	5639.013	5.62	56439.36	5.64	2.844	1003.98
		✓			✓		✓	57.876	16.7	21.21	573.422	5.61	59570.34	5.96	3.465	102.242	57.884	16.62	21.23	5603.478	5.61	56488.21	5.65	3.483	998.26

[1]Values may have been affected by some unknown external factors and should be treated with care.

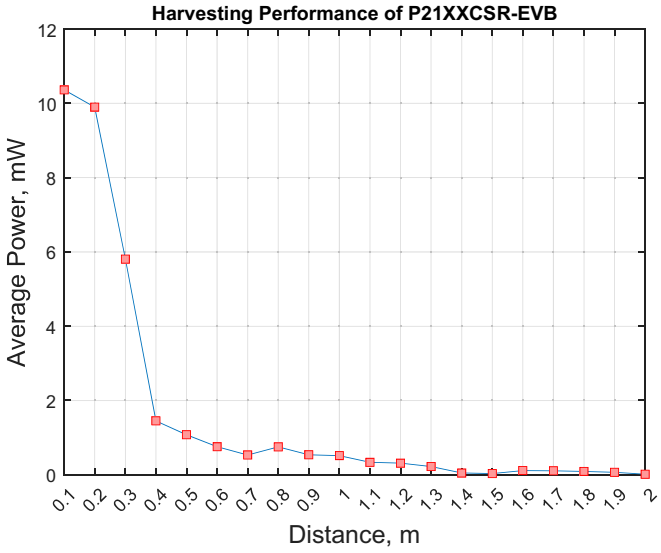

Fig. 6. Energy Harvesting Performance of the WPT receiver over distance (here, distance referees to the distance between the WPT transmitter and WPT receiver's antenna. Power was calculated using the constant 3.3 V output voltage when no load is connected.)

sleep/idle phases. We can see that depending on the number of channels and payload size, the duration of the advertising phase varies from about 2 s to almost 3.5 s. Meanwhile, the total energy consumption in the advertising phase is affected by the number of channels, the payload size, and the transmit power, and varies between about 30 μJ and 78 μJ. Notably, it can be seen that the energy consumption did not linearly change with the change of transmit power.

B. WPT measurement results

Here, we measure the performance of the energy transfer between the Powercast transceiver and receiver versus distance. The measurement results in Fig. 6 show the amount of harvested power. Notice that the collected power drops significantly once the distance increases beyond 30 cm. When the distance between the Powercast receiver and transmitter

TABLE IV
PERFORMANCE OF CAPACITORS CHARGING OVER DISTANCE

Distance (cm)	2200uF Capacitor						50mF Capacitor					
	Sample 1		Sample 2		Sample 3		Sample 1		Sample 2		Sample 3	
	Time (s)	Voltage (mV)	Time (s)	Voltage (mV)	Time (s)	Voltage (mV)	Time (s)	Voltage (mV)	Time (s)	Voltage (mV)	Time (s)	Voltage (mV)
100	0	10	50	590	100	970	0	10	200	106	450	274
90	0	10	50	710	100	1110	0	10	200	346	450	682
80	0	10	25	450	75	1130	0	10	200	434	450	882
70	0	10	25	470	50	830	0	10	200	474	450	970
60	0	10	25	690	50	1190	0	10	200	666	400	1218
50	0	10	25	930	40	1230	0	10	200	1290	450	1850
40	0	10	25	1450	35	1810	0	10	100	1250	200	1690
30	0	10	4	990	11	1850	0	10	50	1490	75	1750
20	0	10	1	990	2.8	1890	0	10	20	1470	30	1930
10	0	10	0.4	990	0.88	2210	0	10	10	1570	13	1990

is about 2 m, only 0.0165 mW is harvested. Interesting, by comparing the results shown in Table III, one can conclude that WPT can provide sufficient energy for a complete BLE transmission, which has an average power consumption below 6 mW, as long as the distance from the RF source is smaller than 0.3 m.

Table IV lists the voltage across the capacitors for three different time instances relative to the start of the experiment. Initially, the voltage across the capacitors at each point is about 10 mV. Once the WPT transmitter is enabled, the voltage at the capacitor increases fairly linearly with time. In case the WPT receiver is placed decently close to the transmitter, the linear increase is followed by a saturation phase, during which the voltage increases slowly until reaching the full-charge level (see, e.g., the results for 10 cm or 40 cm distance and 50 mF capacitor). When the distance is increased, the rate of the voltage growth, and thus the time required for charging the capacitor, is greatly increased.

C. WPT+BLE measurement results

Fig. 7 illustrates the BLE packets captured by Wireshark in BLE advertising channel 37, which we use as one of our performance metrics. Note that we filter out all the received packets originating from devices other than our target BLE

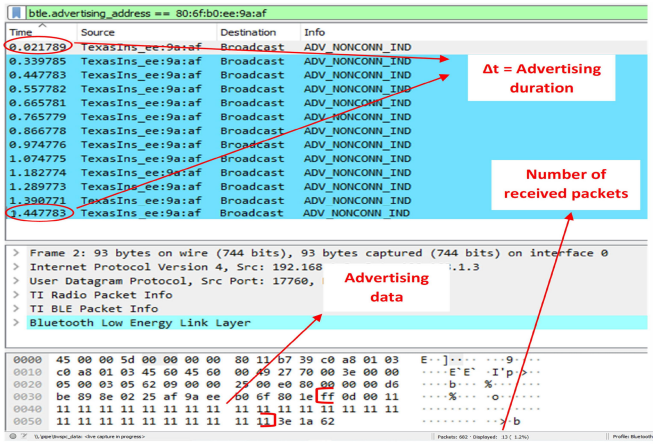

Fig. 7. Wireshark software output (Green line on the top shows the address of the transmitting device. The active phase duration was calculated by taking the time difference between the first and last packets in a burst. The total number of received and displayed packets is shown at the bottom right corner.)

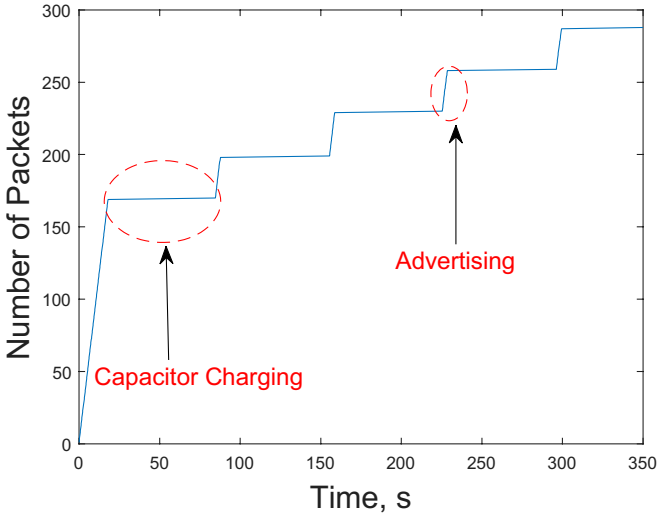

Fig. 8. Number of packets received from WPT-BLE device versus time for the case: single advertising channel, -20 dBm TX power and the minimum advertising data at 100ms advertising interval when the chosen capacitor is 50 mF and the distance between WPT transmitter and receiver is 50 cm.

TABLE V
WPT+BLE TRANSMISSION AT 100MS ADVERTISING INTERVAL

Number of CH			TX Power (dBm)			Packet Size		50mF Capacitor		2200uF Capacitor	
								Duration (s)	Number of Received Packets	Duration (s)	Number of Received Packets
1	2	3	0	5	-20	Min	Max				
✓			✓			✓		22.081551	199	1.880975	17
✓			✓				✓	21.628713	197	1.687978	17
✓				✓		✓		22.027523	195	1.785976	17
✓				✓			✓	21.527715	196	1.674976	16
✓					✓	✓		22.687575	202	2.102971	20
✓					✓		✓	21.861709	201	1.781976	17
	✓		✓			✓		20.852722	184	1.879776	18
	✓		✓				✓	20.776727	190	1.672978	17
	✓			✓		✓		19.356746	172	1.782976	18
	✓			✓			✓	20.143736	186	1.564981	13
	✓				✓	✓		21.562717	196	1.973975	19
	✓				✓		✓	21.275717	186	1.894975	17
		✓	✓			✓		20.823726	189	1.673778	17
		✓	✓				✓	19.769743	178	1.571975	15
		✓		✓		✓		20.392731	185	1.569979	14
		✓		✓			✓	18.938725	171	1.368974	12
		✓			✓	✓		21.373718	186	1.915974	18
		✓			✓		✓	20.682725	186	1.803976	17

transmitter. On average, 188 packets are captured when the WPT receiver is connected to the 50 mF capacitor, while only 16 packets are seized when connected to the 2200 μF capacitor charged to 2 V level. Table V shows the total number of received packets and the time taken to transmit these packets. When measuring these, the WPT transmitter is kept off.

Based on the results in Table V, it is clear that the BLE device configured to its lowest power consumption mode (-20 dBm of TX power, the minimum payload, and one channel) sends the maximum number of packets. Moreover, configuring the BLE device to its maximum power consumption mode results in the lowest duration of operation. Overall, one can also see a good correlation of the results reported in Tables V and III.

Finally, we enable the WPT transmitter and observe the operation of the WPT-BLE integrated system. Fig. 8 illustrates how the number of the packets received from our target device changes in time for one illustrative case. The periodic pattern of operation composing active transmissions (characterized by the increasing number of received packets) and charging (when the power output of the WPT receiver is disabled until the voltage of the capacitor reaches the threshold, thus powering down the BLE transceiver and preventing it from sending packets) can be observed. In the beginning, the capacitor was charged to 2 V, so the number of packets sent at the very beginning of the measurements is higher than that sent in the follow-up phases (recall, that the supply is provided to the BLE device once the voltage on the capacitor exceeds 1.2 V).

Table VI depicts the mean operation time of the charging phase and the following advertising phase at each distance. Note that the 2200 μF capacitor fails to perform the advertising-charging periodic operation once the capacitor falls to the Vmin (1.03 V) when the distance between the RF source and WPT receiver is more than 20 cm. Within a 20 cm distance, it enables a continuous BLE advertising without being discharged. Though the reason for this behavior needs to be studied further, one explanation can be an overly long power-up start procedure of the BLE transceiver. The 50 mF capacitor can perform continuous BLE advertising without being discharged at about 10 cm distance. Interestingly, the trend for capacitor charging time increase with distance is not consistent as the charging time for 40 cm and 80 cm distance was lower than at 30 cm and 70 cm, respectively. We expect that this has been caused by the constructive and destructive effect of the refractions from the various surfaces (e.g., the metal shield covering the cables) in the office environments where the tests were carried out. Note that small-scale fading could be avoided by taking sufficiently large number of samples for averaging.

TABLE VI
WPT+BLE MEAN TIME OF CHARGING AND ADVERTISING PHASES OVER DISTANCE.

Distance	50mF Capacitor		2200uF Capacitor	
	Duration (s)		Duration (s)	
(cm)	Cap. Charging	Advertising	Cap. Charging	Advertising
100	433.52	2.96	Capacitor doesn't recharge to threshold voltage once it falls to Vmin.	
90	152.61	2.57		
80	173.1	3.29		
70	326.21	2.97		
60	275.8	2.98		
50	54.74	2.46		
40	4.84	5.71		
30	14.45	3.4		
20	2.34	18.71	Cap. doesn't discharge to threshold voltage.	
10	Cap. doesn't discharge to threshold voltage.			

V. CONCLUSIONS

WPT is a promising technology to enable un-intermittent and maintenance-free operation of IoT devices. In this paper, we employed empirical methods to study the energy efficiency and performance of state-of-the-art WPT and IoT hardware platforms, namely the Powercast WPT solution and the TI CC2652R1 system-on-chip. Specifically, we first characterized the energy consumption of the CC2652R1 under different BLE communication configurations and the amount of energy the P21XXCSR-EVB can receive from TX91501 WPT transmitter. Then, we merged the two platforms to devise a WPT-powered IoT device communicating over BLE, and studied it. Our results show it is possible to instrument a WPT-powered IoT device today. The BLE technology, characterized by low packet on-air time, low transmission power, decently simple transceiver, and a high level of configurability, is an attractive radio access technology option. At the same time, our results show that without directing the power (e.g., using beamforming or directive antennas), the amount of energy collected from an RF signal is rather limited, specially as the distance increases. For example, for the system investigated in this study and characterized with an average consumption of 5.6-5.8 mW, the non-intermittent operation was possible at a mere 30 cm from the WPT transmitter.

Though we believe that the results reported in this paper can serve as a reference (both for designs and analytic/simulation models), they should, by no means, be treated as the ultimate metric or best-case performance. Indeed, there are multiple opportunities for improvement. Specifically, the power consumption during the sleep/idle state, which is a crucial component for IoT device operation, can be brought down by using more efficient low-power modes of the microcontroller and optimizing the consumption of the peripherals. In future, we plan to perform some optimizations to address this challenge. It is also worth noting that, in this study, we intentionally did not use any application-specific peripherals.

ACKNOWLEDGMENT

The research has been supported by the Erasmus Intern mobility (No. 2020/21-P-132), the Finnish Foundation for Technology Promotion, and Academy of Finland projects MRAT-SafeDrone (decision 341111), FIREMAN (decision 348008), UPRISING (decision 348515) and 6G Flagship program (decision 346208).

REFERENCES

[1] O. L. A. López, H. Alves, R. D. Souza, S. Montejo-Sánchez, E. M. G. Fernández and M. Latva-Aho, "Massive Wireless Energy Transfer: Enabling Sustainable IoT Toward 6G Era," *IEEE Internet Things J.*, vol. 8, no. 11, pp. 8816-8835, 1 June1, 2021, doi: 10.1109/JIOT.2021.3050612.

[2] B. Munir and V. Dyo, "On the Impact of Mobility on Battery-Less RF Energy Harvesting System Performance," *Sensors*, vol. 18, no. 11, p. 3597, Oct. 2018, doi: 10.3390/s18113597.

[3] G. K. Ijemaru, K. L.-M. Ang, and J. K. Seng, "Wireless power transfer and energy harvesting in distributed sensor networks: Survey, opportunities, and challenges," *Int. J. Distrib. Sensor Netw.*, vol. 18, no. 3, p. 155014772110677, Mar. 2022, doi: 10.1177/15501477211067740.

[4] U. Baroudi, A. Qureshi, S. Mekid, and A. Bouhraoua, "Radio Frequency Energy Harvesting Characterization: An Experimental Study," *IEEE 11th Int. Conf. Trust, Security and Privacy in Comput. and Commun.*, Jun. 2012, pp. 1976-1981, doi: 10.1109/trustcom.2012.231.

[5] H. Aboueidah et al., "Characterization of RF energy harvesting at 2.4 GHz," *24th IEEE Int. Conf. Electron., Circuits Syst. (ICECS)*, 2017, pp. 446-449, doi: 10.1109/ICECS.2017.8292118.

[6] Q. Liu, W. IJntema, A. Drif, P. Pawełczak, and M. Zuniga, "BEH: Indoor Batteryless BLE Beacons using RF Energy Harvesting for Internet of Things," *arXiv:1911.03381 [cs, eess]*, Nov. 2019, [Online]. Available: https://arxiv.org/abs/1911.03381.

[7] K. Lee and J. Ko, "RF-Based Energy Transfer Through Packets: Still a Dream? or a Dream Come True?," *IEEE Access*, vol. 7, pp. 163840-163850, 2019, doi: 10.1109/ACCESS.2019.2950711.

[8] J. Tepper et al., "Evaluation of RF Wireless Power Transfer for Low-Power Aircraft Sensors," *AIAA/IEEE 39th Digit. Avionics Syst. Conf. (DASC)*, 2020, pp. 1-6, doi: 10.1109/DASC50938.2020.9256404.

[9] P. Bulić, G. Kojek, and A. Biasizzo, "Data Transmission Efficiency in Bluetooth Low Energy Versions," *Sensors*, vol. 19, no. 17, p. 3746, Aug. 2019, doi: 10.3390/s19173746.

[10] S. Gautam, S. Kumar, S. Chatzinotas and B. Ottersten, "Experimental Evaluation of RF Waveform Designs for Wireless Power Transfer Using Software Defined Radio," *IEEE Access*, vol. 9, pp. 132609-132622, 2021, doi: 10.1109/ACCESS.2021.3115048.

[11] R. La Rosa, C. Dehollain, and P. Livreri, "Advanced Monitoring Systems Based on Battery-Less Asset Tracking Modules Energized through RF Wireless Power Transfer," *Sensors*, vol. 20, no. 11, p. 3020, May 2020, doi: 10.3390/s20113020.

[12] J. Lindh, C. Lee, M. Hernes, and S. Johnsrud, "Measuring CC13xx and CC26xx Current Consumption," Accessed: Jun. 11, 2022. [Online]. Available: https://www.ti.com/lit/an/swra478d/swra478d.pdf?ts=1657467542843.